Journal of Organometallic Chemistry 693 (2008) 2723–2731

Contents lists available at ScienceDirect

Journal of Organometallic Chemistry

journal homepage: www.elsevier.com/locate/jorganchem

From symmetrical to unsymmetrical bimetallic nickel complexes bearing aryl-linked iminopyridines; synthesis, structures and ethylene polymerisation studies

Jérémie D.A. Pelletier, John Fawcett, Kuldip Singh, Gregory A. Solan *

Department of Chemistry, University of Leicester, University Road, Leicester LE1 7RH, UK

ARTICLE INFO

Article history:
Received 16 March 2008
Received in revised form 12 May 2008
Accepted 13 May 2008
Available online 21 May 2008

Keywords:
Nickel
Ethylene polymerisation
Catalyst
Bimetallic
Iminopyridine

ABSTRACT

Both symmetrical and unsymmetrical tetramethylphenyl-linked iminopyridines, 1,4-{(2-C_5H_4N)RC=N}$_2$-2,3,5,6-Me_4C_6 [R = H (L1a), Me (L1b)] and 1-{(2-C_5H_4N)HC=N}-4-{(2-C_5H_4N)MeC=N}-2,3,5,6-Me_4C_6 (L1c), have been prepared in good yield using straightforward condensation strategies. The molecular structures of L1a and L1c reveal the adjacent imino and pyridyl nitrogen atoms to adopt *transoid* configurations. Interaction of L1x with two equivalents of NiX_2 [NiX_2 = (DME)$NiBr_2$ (DME = 1,2-dimethoxyethane), $NiCl_2$] in *n*-BuOH at elevated temperature affords the paramagnetic bimetallic complexes, [(L1x)Ni_2X_4] [L1x = L1a, X = Br (**1a**); L1x = L1b, X = Br (**1b**); L1x = L1c, X = Br (**1c**); L1x = L1a, X = Cl (**1d**)] in moderate to good yield. Adduct formation results on treatment of bromide-containing **1a**–**1c** with DMF (dimethylformamide) to yield dicationic [(L1x)$Ni_2Br_2(DMF)_6$]Br_2 [L1x = L1a (**2a**), L1b (**2b**), L1c (**2c**)], while with chloride-containing **1d** the neutral species [(L1a)$Ni_2Cl_4(DMF)_4$] (**3**) is obtained. Activation of **1a**–**1d** and **2c** with excess methylaluminoxane (MAO) generates active ethylene polymerisation catalysts (**1b**/MAO > **1c**/MAO > **1a**/MAO ~ **1d**/MAO > **2c**/MAO) affording mixtures of waxes and low molecular weight solid polyethylene. Multinuclear NMR and GC analysis of the waxy components reveal methyl branched materials that contain mostly internal unsaturation along with low levels of α-olefins. Broad molecular weight distributions are observed for all the polymers obtained, with that from **1b**/MAO leading to the highest molecular weight. Single crystal X-ray diffraction studies have been performed on L1a, L1c, **2a**–**2c** and **3**.

1. Introduction

Recent years have witnessed a considerable growth in interest in the development and application of known and new compartmental ligands as supports for two catalytically-active metal centres [1–4]. This attention stems, in part, from the potential for cooperative interactions (and unique catalytic behaviour) that may ensue when two metal centres are forced into close proximity. With regard to alkene polymerisation applications, most advances have occurred using early transition metals [5,6] while in recent years the potential for using late transition metal systems [7,8] and combinations of both have been recognised [9].

The pyridylarylimine family of mono-nickel catalysts has provided a thoroughly studied series of group 10 catalysts for the polymerisation of ethylene, allowing access to low molecular weight linear and branched polyethylene [10]. Within the bidentate *N*,*N*-chelating ligand frame (A, Fig. 1), variation in the steric/electronic properties of the *N*-aryl group, the imino-carbon substituent (R) and the pyridyl substituents and their impact on catalytic performance have all been investigated. In contrast, incorporation of two pyridyl-imine binding domains into a binucleating ligand frame has received less attention [11]. For example, dinickel catalysts supported by the methylene-linked pyridylarylimine (B, Fig. 1) have only been recently reported and shown to exhibit high activities for ethylene polymerisation/oligomerisation [11b].

With the intention of bringing the nickel centres into closer proximity, we have targeted aryl-linked pyridylimines (C, Fig. 1) [12] and, in particular, the more sterically demanding tetramethylphenyl-linked derivative [R^1 = Me (L1x)] [13]. In addition, we have been interested in probing the effect that subtle modifications to the two pyridyl-imine binding domains have on catalytic performance. Specifically, the nature of the two imino-carbon substituents (R) in L1x will be systematically varied to incorporate symmetrical aldimine–aldimine [R = H (L1a)] and ketimine–ketimine [R = Me (L1b)] combinations along with the unsymmetrical [R = H, Me (L1c)] counterpart.

* Corresponding author. Tel.: +44 116 252 2096; fax: +44 116 252 3789.
E-mail address: gas8@leicester.ac.uk (G.A. Solan).

0022-328X/$ - see front matter © 2008 Elsevier B.V. All rights reserved.
doi:10.1016/j.jorganchem.2008.05.020

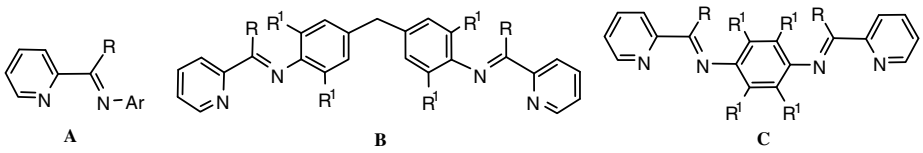

Fig. 1. Pyridylarylimine (A), methylene-linked pyridylarylimine (B) and 1,4-aryl-linked pyridylimine (C); R or R^1 = H or hydrocarbyl.

2. Results and discussion

2.1. Ligand synthesis

Interaction of 1,4-$(NH_2)_2$-2,3,5,6-Me_4C_6 with two equivalents of either 2-pyridinecarboxaldehyde in ethanol at room temperature or with 2-acetylpyridine in *n*-BuOH at 90 °C, in the presence of a catalytic amount of formic acid, gave 1,4-{(2-C_5H_4N)RC=N}$_2$-2,3,5,6-Me_4C_6 [R = H (L1a), Me (L1b)] in good yields, respectively (Scheme 1). Unsymmetrical L1c can be accessed in two steps by firstly treating 1,4-$(NH_2)_2$-2,3,5,6-Me_4C_6 with one equivalent of 2-acetylpyridine to give 1-(2-C_5H_4N)MeC=N(2,3,5,6-Me_4C_6-4-NH_2) (I) and secondly reacting I with 2-pyridinecarboxaldehyde. L1a–L1c have been characterised by ^{1}H NMR, ^{13}C NMR and IR spectroscopy along with electrospray mass spectrometry (see Section 4). In addition, L1a and L1c have been the subject of single crystal X-ray diffraction studies.

Yellow crystals of L1a and L1c suitable for the single crystal X-ray determinations were grown from concentrated ethanol or chloroform solutions, respectively. The structures are similar and will be discussed together. A perspective view of L1a is shown in Fig. 2; selected bond lengths and angles for both L1a and L1c are listed in Table 1. The structures consist of two terminal iminopyridyl units bridged by a 2,3,5,6-tetramethylphenyl moiety with an inversion centre located within the respective central aryl groups. In the case of L1c, the imino-carbon substituents are disordered between hydrogen and methyl in a 50:50 ratio. Each pyridyl-imine section is nearly planar [*tors.* N(1)–C(5)–C(6)-N(2) 11.9° (L1a) 5.7° (L1c)] with the imine and pyridine nitrogen atoms disposed in a *trans* configuration. The central aryl rings adopt a quasi-orthogonal arrangement with respect to the pyridyl-imine units [*tors.* C(6)–N(2)–C(7)–C(8) 113.0° (L1a), 105.4° (L1c)] in a manner similar to that observed for 1,4-{(2-C_5H_4N)HC=N}$_2C_6H_4$ [14].

In the mass spectra for L1a–L1c, peaks corresponding to the protonated forms of their molecular ions are evident while in their IR spectra υ(C=N) bands for the imine units are observed in the range 1631–1641 cm^{-1}. The ^{13}C NMR spectra for L1a and L1b reveal in each the presence of only one downfield signal for the equivalent imino-carbon atoms while for L1c two signals are apparent for the independent aldimine and ketimine carbon atoms. The C*H*=N and C*Me*=N protons in L1a and L1b fall in the typical chemical shift ranges while in L1c signals for both types of proton are seen as singlets at δ 8.30 and δ 2.11, respectively.

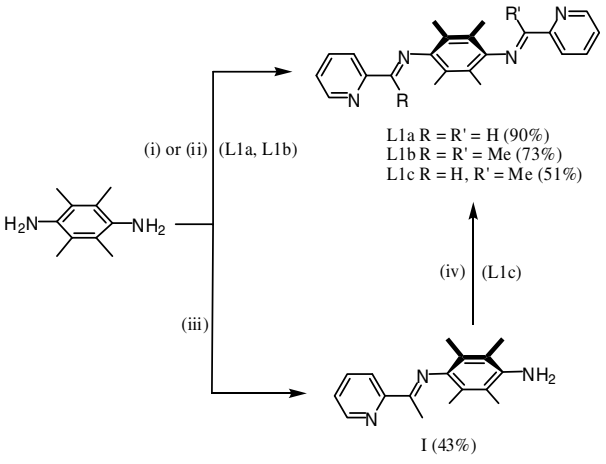

Scheme 1. Reagents and conditions: (i) 2.2 eq. (2-C_5H_4N)CHO, EtOH, H^+ (cat.), RT; (ii) 2.2 eq. (2-C_5H_4N)CMeO, *n*-BuOH, H^+ (cat.), 90 °C; (iii) 0.7 eq. (2-C_5H_4N)CMeO, toluene, H^+ (cat.), 50 °C; (iv) 1.1 eq. (2-C_5H_4N)CHO, EtOH, H^+ (cat.), RT.

2.2. Synthesis of complexes

Reaction of two equivalents of (DME)$NiBr_2$ with L1a–L1c in *n*-butanol at 100 °C overnight gave [(L1x)Ni_2Br_4] [L1x = L1a (**1a**), L1b (**1b**), L1c (**1c**)] in good yield, respectively (Scheme 2). Similarly, treatment of $NiCl_2$ with L1a in *n*-butanol yielded [(L1a)Ni_2Cl_4] (**1d**)

Table 1
Selected bond lengths (Å) and angles (°) for L1a and L1c

	L1a	L1c
Bond lengths		
N(1)–C(1)	1.334(2)	1.339(3)
N(1)–C(5)	1.336(2)	1.341(2)
N(2)–C(6)	1.255(2)	1.267(2)
N(2)–C(7)	1.421(2)	1.429(2)
C(5)–C(6)	1.459(2)	1.486(3)
Bond angles		
C(6)–N(2)–C(7)	117.89(14)	120.23(16)
N(1)–C(5)–C(6)	114.26(15)	115.29(18)
N(2)–C(6)–C(5)	122.99(16)	118.89(18)

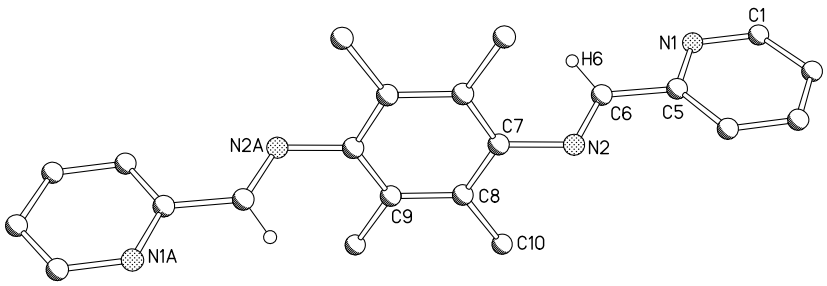

Fig. 2. Molecular structure of L1a; all hydrogen atoms, apart for H6, have been omitted for clarity. Atoms with suffix A are generated by symmetry (1 − *x*, −*y*, 2 − *z*).

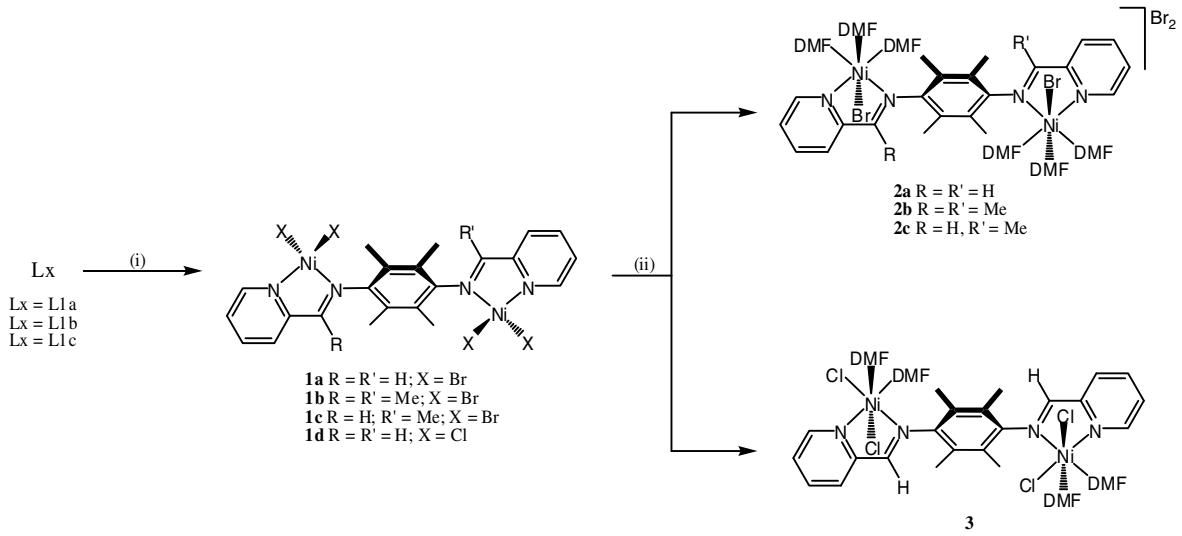

Scheme 2. Reagents and conditions: (i) 2 eq. NiX_2 [NiX_2 = (DME)$NiBr_2$ or $NiCl_2$], *n*-BuOH, 100 °C and (ii) xs. DMF, 90 °C.

in good yield. Complexes **1a**–**1d** have been characterised by FAB mass spectrometry, IR spectroscopy and by magnetic susceptibility measurements (see Table 2 and Section 4). In addition, the DMF adducts of **1a**–**1d** (**2a**–**2c** and **3**) have been crystallographically characterised (*vide infra*).

The FAB mass spectrometric data for **1a**–**1d** exhibit characteristic mass and isotope distributions with fragmentation peaks consistent with the loss of one or more halide ions. As with [aryliminopyridine]NiX_2 complexes [10c,10f], bimetallic **1a**–**1d** are all paramagnetic and display magnetic moments ranging from 3.9 to 4.1 μ_B, consistent with the presence of two non-interacting high spin Ni(II) centres (using $\mu^2 = \sum \mu_i^2$, where μ_i is the magnetic moment of the individual metal centres) [15]. The IR spectra for **1a**–**1d** show absorption bands around 1595 cm^{-1} which correspond to υ(C=N) absorption bands for coordinated imines and are shifted by *ca.* 40 cm^{-1} in comparison with the free ligands L1a–L1c.

Due to the insolubility of **1a**–**1d** in a range of common organic solvents (*e.g.*, CH_2Cl_2, MeCN, and $CHCl_3$), recrystallisation proved problematic. However, dissolution of **1a**–**1d** in warm DMF could be achieved and layering of the cooled solutions with diethyl ether gave [(L1x)$Ni_2Br_2(DMF)_6$]Br_2 [L1x = L1a (**2a**), L1b (**2b**), L1c (**2c**)] and [(L1a)$Ni_2Cl_4(DMF)_4$] (**3**) (Scheme 2) as orange crystals that proved suitable for single crystal X-ray diffraction studies.

The structures of **2a** and **2b** are similar and will be discussed together. A representation of **2b** is depicted in Fig. 3; selected bond lengths and angles for both complexes are listed in Table 3. The structures of both complexes are based on a centro-symmetrical bimetallic nickel-containing dicationic unit and charge balanced by two non-coordinating bromide anions. Within the cationic unit, L1x [L1a (**2a**), L1b (**2b**)] acts as a bis(bidentate) ligand with the nickel centres forming five-membered chelate rings with the two pyridyl-imine units. The coordination spheres at each metal centre are completed by three oxygen-bound DMF ligands and one bromide ligand so as to give distorted octahedral geometries. Two DMF ligands are disposed *trans* to the pyridyl and imine nitrogen donors while the third one is *trans* to the bromide. In both structures, the N–metal bond distances show similar characteristics with the Ni–$N_{pyridine}$ bond being shorter [Ni(1)–N(1) 2.040(3) Å (**2a**), 2.039(4) Å (**2b**)] than the corresponding Ni–N_{imine} bond [Ni(1)–N(2) 2.119(3) Å (**2a**), 2.112(4) Å (**2b**)], consistent with the better donor capability of a pyridine over an imine [16]. This relative donor capability is also reflected in the corresponding *trans* metal–oxygen bond distances with Ni(1)–O(3) for **2a** [2.149(6) Å] being longer than Ni(1)–O(1) [2.023(3) Å]. A similar trend is also observed for **2b** but the variation of the distance is less significant [Ni(1)–O(3) 2.042(3) Å *vs.* Ni(1)–O(1) 2.032(3) Å]. The central aryl groups are oriented almost orthogonally to the pyridyl-imine units [*tors.* Ni(1)–N(2)–C(7)–C(8) 106.5° (**2a**), Ni(1)–N(2)–C(7)–C(8) 103.3° (**2b**)] with the result that the aryl *o*-methyl groups point in a similar direction to the *trans* disposed bromide and DMF ligands. The two nickel centres are located slightly closer in **2b** [at 8.786 Å] when compared to **2a** [at 8.897 Å]. No intermolecular interactions of note are apparent.

The X-ray data for **2c** were solved in two different space groups, *viz.* $P\bar{1}$ and *P*1. In $P\bar{1}$ (the preferred solution) a centro-symmetrical dicationic unit similar to that seen for in **2a** and **2b** was revealed but with a disordered methyl/hydrogen (50:50) acting as the substituent for each of the two imino-carbon atoms (*cf.*, L1c). In *P*1, however, the inequivalent nature of the imino group substituents was confirmed in the form of two aldimine–ketimine-containing enantiomers. A perspective view of one of the enantiomers in **2c** (in *P*1) is shown in Fig. 4; selected bond distances and angles are listed for both crystallographic solutions in Table 4. The general structural features of **2c** are similar to that seen in **2a** and **2b** with a dicationic dinickel unit counter balanced by two bromide anions

Table 2
Selected characterisation data for **1a**–**1d**

Complex	Colour	FAB mass spectra	υ(C=N)[a] (cm^{-1})	μ_{eff}[b] (μ_B)
1a	Pale green-orange	699 $[M-Br]^+$, 620 $[M-2Br]^+$, 538 $[M-3Br]^+$	1595	4.2
1b	Pale orange	727 $[M-Br]^+$, 645 $[M-2Br]^+$, 567 $[M-3Br]^+$	1595	3.9
1c	Pale orange	$[M-Br]^+$, 633 $[M-2Br]^+$, 553 $[M-3Br]^+$	1597	3.9
1d	Pale orange	666 $[M-Cl]^+$, 530 $[M-2Cl]^+$, 495 $[M-3Cl]^+$	1595	4.0

[a] Recorded on a Perkin–Elmer Spectrum One FT-IR spectrometer on solid samples.
[b] Recorded on an Evans balance at ambient temperature.

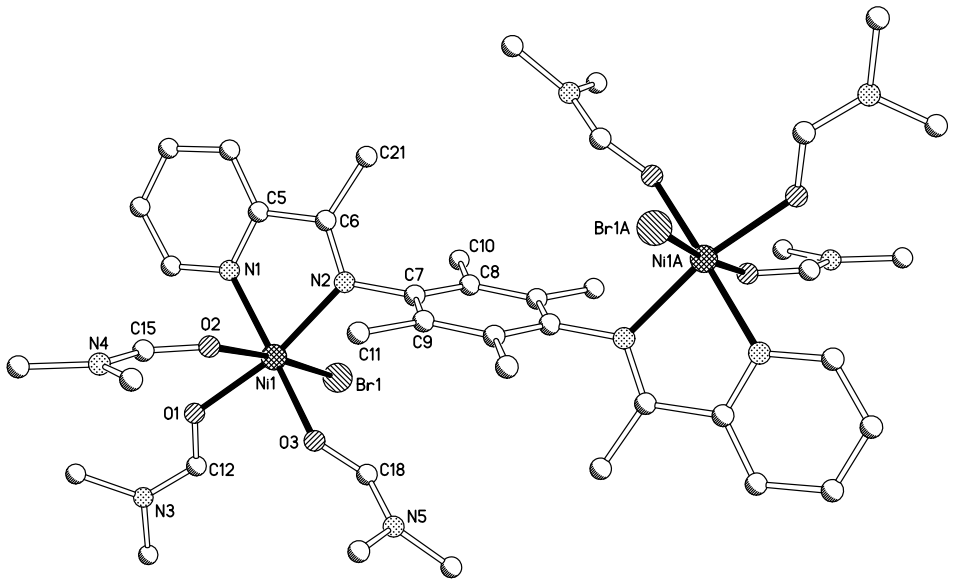

Fig. 3. Molecular structure of the dicationic unit in **2b**; all hydrogen atoms have been omitted for clarity. Atoms with suffix A are generated by symmetry ($-x+1$, $-y+1$, $-z+1$).

Table 3
Selected bond lengths (Å) and angles (°) for **2a** and **2b**

	2a	2b
Bond lengths		
Ni(1)–N(1)	2.040(3)	2.039(4)
Ni(1)–N(2)	2.119(3)	2.112(4)
Ni(1)–Br(1)	2.4956(8)	2.5377(8)
Ni(1)–O(1)	2.023(3)	2.032(3)
Ni(1)–O(2)	2.103(3)	2.123(3)
Ni(1)–O(3)	2.149(6)	2.042(3)
C(6)–N(2)	1.271(5)	1.280(6)
C(6)–C(21)	–	1.495(6)
Bond angles		
N(1)–Ni(1)–N(2)	79.06(13)	78.42(15)
N(1)–Ni(1)–Br(1)	94.00(9)	96.20(11)
N(1)–Ni(1)–O(1)	92.06(13)	91.87(14)
N(1)–Ni(1)–O(2)	87.25(13)	85.74(13)
N(1)–Ni(1)–O(3)	167.62(16)	168.50(14)
N(2)–Ni(1)–O(1)	169.53(13)	169.25(14)
N(2)–Ni(1)–O(2)	90.81(12)	91.54(13)
N(2)–Ni(1)–O(3)	100.13(15)	97.45(14)
N(2)–Ni(1)–Br(1)	93.33(9)	93.77(10)
O(1)–Ni(1)–O(2)	83.17(12)	83.04(13)
O(1)–Ni(1)–O(3)	87.35(16)	91.19(13)
O(1)–Ni(1)–Br(1)	92.82(10)	91.86(10)
O(2)–Ni(1)–O(3)	80.40(16)	83.63(13)
O(2)–Ni(1)–Br(1)	175.84(8)	174.61(9)
O(3)–Ni(1)–Br(1)	8.38(13)	94.78(10)

with the relative disposition of the donor atoms within the cation the same as in its symmetrical counterparts. Inspection of the N–metal bond distances reveals similar characteristics for both nickel centres; for example the Ni–$N_{pyridine}$ bonds are shorter [Ni(1)–N(1) 2.042(4) Å] than the Ni–N_{imine} [Ni(1)–N(2) 2.126(4) Å] ones.

The molecular structure of **3** is shown in Fig. 5; bond lengths and angles are collected in Table 5. The main difference between **3** and **2** is that the bimetallic unit is now overall neutral. In **3**, the symmetrical 1,4-bis(aldiminopyridinyl)aryl ligand L1a again acts as a bis(bidentate) ligand but the nature of the monodentate ligands coordinated to each nickel centre varies when compared to **2**. Thus, each nickel centre is bound to two chlorides and two oxygen-bound DMF ligands with each pair being disposed mutually *cis*. One DMF-oxygen atom [O(2)] is *trans* to a chloride [Cl(1)] while the other oxygen [O(1)] is *trans* to a pyridine nitrogen atom [N(1)] so as to complete a distorted octahedral geometry. The metal–chlorine distances in **3** are different with Ni(1)–Cl(1) being longer than Ni(1)–Cl(2) [2.4081(10) Å *vs.* 2.3812(9) Å], presumably due to the nature of the ligand *trans* to each. As with **2**, the Ni–$N_{pyridine}$ bond lengths are shorter than the Ni–N_{imine} distances [Ni(1)–N(1) 2.039(2) *vs.* Ni(1)–N(2) 2.150(2)]. The chelate bite angle N(1)–Ni(1)–N(2) [at 79.49(9)°] in **3** is slightly bigger than the corresponding angle in **2a** [at 79.06(13)°].

In the FAB mass spectra for **2a**–**2c** and **3**, fragmentation peaks corresponding to loss of halide ligands from a species devoid of DMF ligands are evident. In the IR spectra, the imine bands could be seen at *ca.* 1595 cm^{-1} with a strong additional band at *ca.* 1644 cm^{-1} which can be ascribed to the C=O absorption bands of the coordinated DMF ligands.

2.3. Screening for ethylene polymerisation

The bimetallic complexes **1a**–**1d** and **2c** have been screened as precatalysts for the polymerisation of ethylene; the results are compiled in Table 6. Typically, a complex was suspended in toluene and treated with 800 equivalents (400 per metal centre) of methylaluminoxane (MAO) at room temperature, ethylene gas (1 bar) was then introduced over a period of 60 min. All the systems were active catalysts affording both polymeric materials and toluene-soluble oligomeric waxes. The activities of the five systems fall in a similar range with the ketimine–ketimine system **1b**/MAO at the top at 409 $g/mmol^{-1}\ h^{-1}\ bar^{-1}$ (run 2) and the **2c**/MAO the bottom (run 5) with the ratio of oligomer to polymer ranging 4:1 for **1b**/MAO to 1:4 for **1d**/MAO.

The ^1H NMR spectra of the oligomeric materials from each run are similar revealing the presence of low levels of α-olefins (13–20%), di-substituted oligomers (79–87%) and trace amounts of tri-substituted and vinylidene chain ends along with an enhanced degree of methyl chain ends. In their ^{13}C NMR spectra, an envelope of peaks around δ 19.9 is consistent with the presence of predominantly methyl branches [17]; trace levels of longer chain branches (*e.g.*, ethyl and propyl) are also evident. The GC spectra support this broad range of oligomeric microstructures with multiple peaks found in addition to those corresponding to the linear α-olefins (in the C10–C30 range). Indeed, this type of branched material is very similar to that found for monometallic pyridyl-imine-nickel

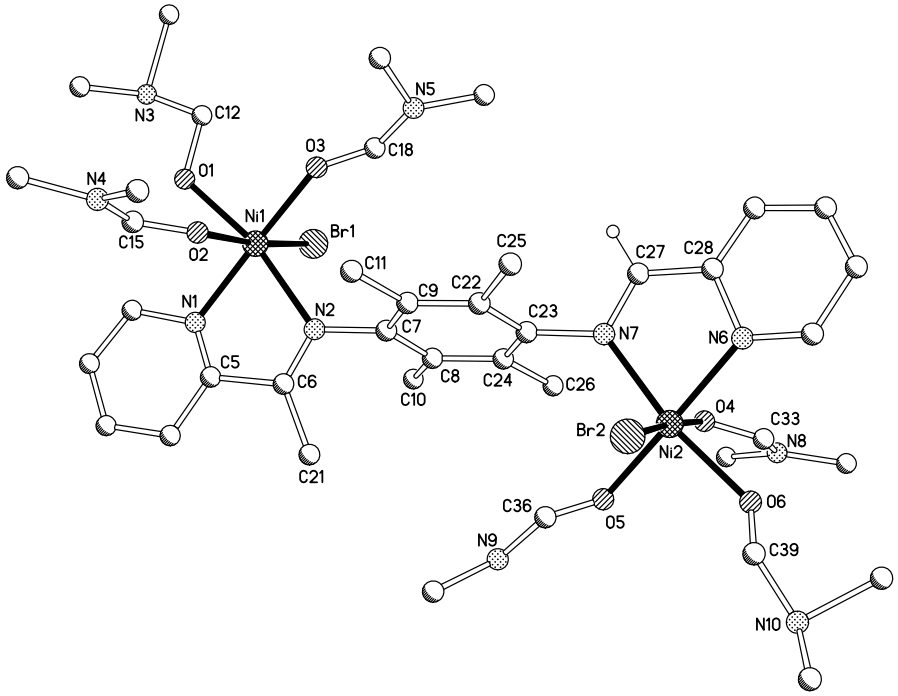

Fig. 4. Molecular structure of **2c**; all hydrogen atoms, apart from H27, have been omitted for clarity.

Table 4
Selected bond lengths (Å) and angles (°) for **2c**

	In $P\bar{1}$	In $P1$
Bond lengths		
Ni(1)–N(1)	2.042(4)	2.015(12)
Ni(1)–N(2)	2.126(4)	2.137(10)
Ni(1)–Br(1)	2.5245(8)	2.541(2)
Ni(1)–O(1)	2.037(4)	2.013(10)
Ni(1)–O(2)	2.112(3)	2.123(10)
Ni(1)–O(3)	2.030(4)	2.046(10)
C(6)–C(21)	1.388(13)	1.465(19)
C(6)–N(2)	1.275(6)	1.224(17)
Ni(2)–N(6)	–	2.076(11)
Ni(2)–N(7)	–	2.105(12)
Ni(2)–Br(2)	–	2.505(2)
Ni(2)–O(4)	–	2.114(9)
Ni(2)–O(5)	–	2.005(10)
Ni(2)–O(6)	–	2.049(10)
C(27)–N(7)	–	1.297(15)
Bond angles		
N(1)–Ni(1)–N(2)	78.88(17)	78.5(4)
N(1)–Ni(1)–Br(1)	95.81(12)	94.0(3)
N(1)–Ni(1)–O(1)	90.98(18)	90.0(5)
N(1)–Ni(1)–O(2)	86.36(14)	88.6(4)
N(1)–Ni(1)–O(3)	169.12(16)	170.4(4)
N(2)–Ni(1)–O(1)	169.03(16)	167.8(4)
N(2)–Ni(1)–O(2)	91.30(13)	92.6(4)
N(2)–Ni(1)–O(3)	97.06(14)	96.3(4)
N(2)–Ni(1)–Br(1)	93.48(10)	93.3(3)
O(1)–Ni(1)–O(2)	83.84(13)	83.1(4)
N(6)–Ni(2)–N(7)	–	77.9(5)
N(6)–Ni(2)–Br(2)	–	97.7(4)
N(6)–Ni(2)–O(4)	–	83.9(4)
N(6)–Ni(2)–O(5)	–	167.3(5)
N(6)–Ni(2)–O(6)	–	92.9(5)
N(7)–Ni(2)–O(4)	–	89.9(4)
N(7)–Ni(2)–O(5)	–	98.2(4)
N(7)–Ni(2)–O(6)	–	169.6(4)
N(7)–Ni(2)–Br(2)	–	93.6(3)
O(4)–Ni(2)–O(5)	–	84.0(4)

catalysts with a chain-walking mechanism being used to account for the observed isomerisation/branching [9,12c].

Several points emerge from inspection of the GPC data for the polymeric components. Firstly, all the systems produce low molecular weight polyethylene with broad molecular weight distributions. Secondly, the aldimine–aldimine systems **1a**/MAO (run 2) and **1d**/MAO (run 4) afford the lowest molecular weight (M_w = 5687 and 3729) polymers. Thirdly, the mixed ketimine–aldimine system **1c**/MAO (run 3) gives the broadest molecular weight distribution (M_w/M_n = 12.2) but notably shows some similarity to the polymer obtained using its DMF adduct as the precatalyst (run 5) and indeed **1b**/MAO (run 2).

Overall, it would appear the nature of the imino-carbon substituent (Me *vs.* H) in these bimetallic systems (**1**/MAO) most clearly affects the activities of the catalysts with the more ketimine content (**1b**/MAO) leading to the most productive system. Small variations are also apparent with regard to the molecular weight characteristics of the polymeric fraction with lower molecular weight product produced with more aldimine content. Use of the DMF adduct of **1c**, **2c**, also allows for an active catalyst albeit one displaying lower productivities to its parent; this latter observation may possibly be due to the competition of DMF and ethylene for a vacant coordination site on nickel in the active catalyst.

3. Conclusions

Tetramethylphenyl-linked iminopyridines have been successfully used as supports for two polymerisation-active nickel centres. Complexes containing combinations of aldimine/aldimine (**1a**, **1d**), ketimine/ketimine (**1b**) and aldimine–ketimine (**1c**) for the two iminopyridine moieties can all be prepared. Derivatisation with DMF allows access, depending on halide substituent, to crystalline salts (**2a**–**2c**) and neutral species (**3**). Combinations of **1**/MAO are all active catalysts for the polymerisation of ethylene affording low molecular weight polyethylene. No significant differences are apparent with regard to the polymer product obtained in each case with catalytic activity being found to follow the order: **1b**/MAO > **1c**/MAO > **1a**/MAO > **2c**/MAO.

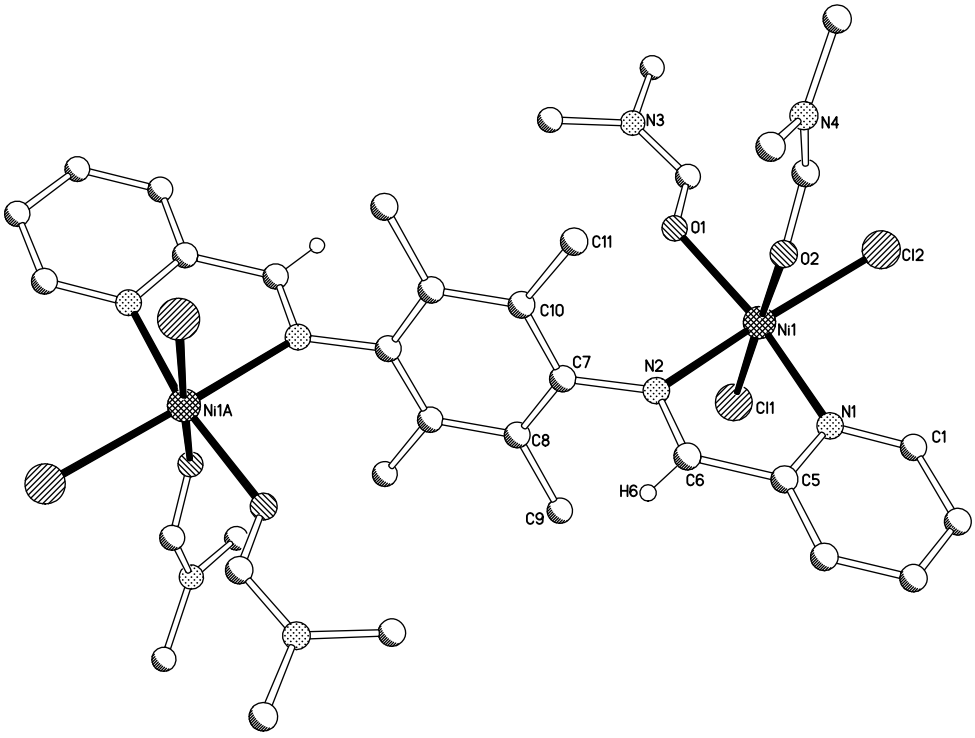

Fig. 5. Molecular structure of **3**; all the hydrogen atoms, apart from H6, have been omitted for clarity. Atoms with suffix A are generated by symmetry (1.5 − *x*, 0.5 − *y*, 2 − *z*).

Table 5
Selected bond lengths (Å) and angles (°) for **3**

Bond lengths			
Ni(1)–N(1)	2.039(2)	Ni(1)–O(1)	2.051(2)
Ni(1)–N(2)	2.150(2)	Ni(1)–O(2)	2.136(2)
Ni(1)–Cl(1)	2.4081(10)	C(6)–N(2)	1.261(3)
Ni(1)–Cl(2)	2.3812(9)		
Bond angles			
N(1)–Ni(1)–N(2)	79.49(9)	N(2)–Ni(1)–Cl(1)	91.86(7)
N(1)–Ni(1)–Cl(1)	89.02(8)	O(1)–Ni(1)–O(2)	88.33(9)
N(1)–Ni(1)–Cl(2)	95.17(7)	O(1)–Ni(1)–Cl(1)	94.95(7)
N(1)–Ni(1)–O(1)	168.95(9)	O(1)–Ni(1)–Cl(2)	94.70(6)
N(1)–Ni(1)–O(2)	87.14(9)	O(2)–Ni(1)–Cl(1)	175.21(6)
N(2)–Ni(1)–O(1)	90.06(8)	O(2)–Ni(1)–Cl(2)	87.55(7)
N(2)–Ni(1)–O(2)	84.63(9)	Cl(1)–Ni(1)–Cl(2)	95.65(4)
N(2)–Ni(1)–Cl(2)	170.72(7)		

Table 6
Catalytic evaluation of **1a**–**1d** and **2c** for ethylene polymerisation[a]

Run	Precat.[b]	Mass of oligomer (g)	Mass of polymer (g)	Activity[c] (g/mmol^{-1} h^{-1} bar^{-1})	M_w[d]	M_n[d]	M_w/M_n[d]
1	**1a**	0.60	1.150	175	5867	823	7.1
2	**1b**	3.30	0.788	409	25716	2569	10.0
3	**1c**	0.80	1.623	242	30770	2526	12.2
4	**1d**	0.40	1.582	198	3729	1533	2.4
5	**2c**	0.40	0.888	129	24276	2448	9.9

[a] General conditions: Toluene (40 ml), 25 °C, reaction time 1 h, 400 eq. MAO per metal centre, ethylene pressure 1 bar (100 kPa), reaction quenched with dilute HCl.
[b] 0.01 mmol employed.
[c] Based on the sum of the mass of oligomer + mass of polymer.
[d] Determined by GPC at 160 °C for polymeric components.

4. Experimental

4.1. General

All operations, unless otherwise stated, were carried out under an inert atmosphere of dry, oxygen-free nitrogen using standard Schlenk and cannular techniques or in a nitrogen purged glove box. Solvents were distilled under nitrogen from appropriate drying agents and degassed prior to use [18] or were employed directly from a Solvent Purification System (Innovative Technology Inc.). The electrospray (ES) mass spectra were recorded using a micromass Quattra LC mass spectrometer with dichloromethane or methanol as the matrix. FAB mass spectra (including high resolution) were recorded on Kratos Concept spectrometer with NBA as matrix. The infrared spectra were recorded in the solid state with Universal ATR sampling accessories on a Perkin–Elmer Spectrum One FTIR instrument. NMR spectra were recorded on a Bruker ARX 250/300 MHz spectrometer (^{1}H) and 62.9/75 MHz (^{13}C); chemical shifts (ppm) are referred to the residual protic solvent peaks and coupling constants are expressed in Hertz (Hz). The high temperature GPC analysis were performed on a PL-220 instrument equipped with two mixed bed – C Columns (Polymer Laboratory) and a refractive index detector. Analyses were undertaken using 1,2,4-trichlorobenzene as solvent at 160 °C and the M_ws were calculated using a universal calibration curve based on polystyrene standards using Easycal PS-2 (Polymer Laboratory). Oligomer products were analysed by GC, using a Perkin–Elmer Autosystem XL chromatograph equipped with a flame ionisation detector and 30m PE-5 column (0.25 mm thickness), injector temperature 45 °C and the following temperature programme: 45 °C/7 min, 45–195 °C/10 °C min^{-1}, 195 °C/5 min, 195–225 °C/10 °C min^{-1}, 225 °C/5 min, 225–250 °C/10 °C min^{-1}, 250 °C/22 min. Magnetic susceptibility studies were performed using an Evans Balance (Johnson Matthey) at room temperature. The magnetic moments were calculated following standard methods [19] and corrections for underlying diamagnetism were applied to the data [20]. Melting points (m.p.) were measured on a Gallenkamp melting point apparatus (model MFB-595) in open capillary tubes and were uncorrected. Elemental analyses were performed at the Science Technical Support Unit, London Metropolitan University.

The reagents 2-pyridinecarboxaldehyde, 2-acetylpyridine, 2,3,5,6-tetramethyl-benzene-1,4-diamine were purchased from Al-

drich Chemical Co. and used without further purification. Nickel dichloride, nickel dibromide 1,2-dimethoxyethane were purchased from Aldrich Chemical Co. and were stored and employed under a dry, oxygen-free nitrogen atmosphere. All other chemicals were obtained commercially and used without further purification.

4.2. Preparation of ligands (L1a–L1c)

4.2.1. N,N′-Bis((pyridin-2-yl)methylene)-2,3,5,6-tetramethylbenzene-1,4-diamine (L1a)

To a suspension of 2,3,5,6-tetramethyl-benzene-1,4-diamine (1.500 g, 9.15 mmol) in absolute ethanol (100 ml) was added 2-pyridinecarboxaldehyde (1.9 ml, 0.02 mol, 2.2 eq.) followed by one drop of formic acid. After stirring overnight at room temperature, the suspension was filtered, washed with cold ethanol and dried under reduced pressure to give L1a in good yield as a pale yellow solid (2.812 g, 90%). Compound L1a: ES mass spectrum, *m*/*z* 343 $[M+H]^+$; FABMS Calc. for $C_{24}H_{22}N_4$, found 343.19225, requires 343.19227; IR (cm^{-1}): 1636 (s), 1585 (w), 1564 (w), 1469 (m), 1438 (m), 1258 (m), 1223 (m), 1146 (w), 1040 (m), 989 (m), 777 (s); ^1H NMR ($CDCl_3$, 293 K): δ 2.01 (s, 12H, Ar-CH_3), 7.34 (ddd, $^3J_{H-H}$ 4.6, 7.6, $^4J_{H-H}$ 1.2, 2H, Py-H), 7.78 (dddd, $^3J_{H-H}$ 7.6, 7.9, $^4J_{H-H}$ 0.8, 0.9, 2H, Py-H), 8.28 (s, 2H, HC=N), 8.31 (ddd, $^3J_{H-H}$ 7.9, $^4J_{H-H}$ 0.8, 0.9, 2H, Py-H), 8.68 (ddd, $^3J_{H-H}$ 4.7, $^4J_{H-H}$ 0.8, 0.9, 2H, Py-H); ^{13}C {^1H} NMR ($CDCl_3$, 293 K): δ 15.0 (CH_3), 121.2 (Ar), 123.5 (Ar), 125.2 (Ar), 136.7 (Ar), 147.2 (Ar), 149.6 (Ar), 154.6 (Ar), 163.8 (C=N); m.p. = 228 °C.

4.2.2. N,N′-Bis(1-(pyridin-2-yl)ethylidene)-2,3,5,6-tetramethylbenzene-1,4-diamine (L1b)

To a mixture of 2,3,5,6-tetramethyl-benzene-1,4-diamine (0.500 g, 3.05 mmol) and 2-acetylpyridine (0.75 ml, 6.71 mmol, 2.2 eq.) in *n*-butanol (50 ml) was added three drops of formic acid. After stirring the reaction mixture at 90 °C overnight, the resulting suspension was filtered, washed with cold ethanol and dried under reduced pressure to give L1b in good yield as a yellow solid (0.823 g, 73%). Compound L1b: ES mass spectrum, *m*/*z* 371 $[M+H]^+$; FABMS Calc. for $C_{24}H_{27}N_4$, found 371.22352, requires 371.22357; IR (cm^{-1}): 1642 (s), 1585 (w), 1561 (w), 1462 (m), 1430 (m), 1359 (m), 1299 (m), 1260 (m), 1102 (w), 1087 (m), 1069 (m), 1041 (w), 992 (m), 745 (s); ^1H NMR ($CDCl_3$, 293 K): δ 1.99 (s, 12H, Ar-CH_3), 2.19 (s, 6H, (CH_3)C=N), 7.35 (ddd, $^3J_{H-H}$ 4.6, 7.6, $^4J_{H-H}$ 1.2, 2H, Py-H), 7.83 (dddd, $^3J_{H-H}$ 7.6, 7.9, $^4J_{H-H}$ 0.8, 0.9, 2H, Py-H), 8.36 (ddd, $^3J_{H-H}$ 7.9, $^4J_{H-H}$ 0.8, 0.9, 2H, Py-H), 8.69 (ddd, $^3J_{H-H}$ 4.7, $^4J_{H-H}$ 0.8, 0.9, 2H, Py-H); ^{13}C {^1H} NMR ($CDCl_3$, 293 K): δ 14.8 (Ar-CH_3), 17.0 (CH_3), 121.6 (Ar), 125.1 (Ar), 136.8 (Ar), 144.8 (Ar), 149.0 (Ar), 157.2 (Ar), 168.3 (C=N); m.p. = 206 °C.

4.2.3. N-(1-(Pyridin-2-yl)ethylidene)-N′-((pyridin-2-yl)methylene)-2,3,5,6-tetramethylbenzene-1,4-diamine (L1c)

L1c can be prepared in two steps: (i) To a mixture of 2,3,5,6-tetramethyl-benzene-1,4-diamine (0.615 g, 0.37 mmol) and 2-acetylpyridine (0.30 ml, 0.27 mmol, 0.7 eq.) in toluene (2 ml) was added two drops of formic acid. The suspension was stirred and heated for three days at 50 °C. On cooling to room temperature, the dark reddish suspension was filtered and washed with cold toluene. The filtrate was evaporated, dissolved in chloroform (2 ml) and cooled to −78 °C for 0.5 h before being filtered. Hexane was added to the filtrate and all volatiles were removed under reduced pressure to give *N*-(1-(pyridin-2-yl)ethylidene)-2,3,5,6-tetramethylbenzene-1,4-diamine (I) as a brown solid (0.310 g, 43%). Compound I: ES mass spectrum, *m*/*z* 268 $[M+H]^+$; IR (cm^{-1}) 3378 (N–H), 1632 (C=N); ^1H NMR ($CDCl_3$, 293 K): δ 1.99 (s, 6H, Ar-CH_3), 2.11 (s, 3H, (CH_3)C=N), 2.13 (s, 6H, Ar-CH_3), 3.40 (s, br, 2H, NH_2), 7.35 (ddd, $^3J_{H-H}$ 4.6, 7.6, $^4J_{H-H}$ 1.2, 1H, Py-H), 7.78 (dddd, $^3J_{H-H}$ 7.6, 7.9, $^4J_{H-H}$ 0.8, 0.9, 1H, Py-H), 8.28 (ddd, $^3J_{H-H}$ 7.9, $^4J_{H-H}$ 0.8, 0.9, 1H, Py-H), 8.69 (ddd, $^3J_{H-H}$ 4.7, $^4J_{H-H}$ 0.8, 0.9, 1H, Py-H); ^{13}C {^1H} NMR ($CDCl_3$, 293 K): δ 14.0 (Ar-CH_3), 15.0 (Ar-CH_3), 17.0 ((CH_3)C=N), 119.2 (Ar), 121.6 (Ar), 122.0 (Ar), 125.0 (Ar), 136.8 (Ar), 138.7 (Ar), 141.4 (Ar), 148.9 (Ar), 157.3 (Ar), 168.1 (C=N); m.p. = 112 °C.

(ii) To a solution of I (0.250 g, 0.94 mmol) in absolute ethanol (10 ml) was added 2-pyridinecarboxaldehyde (0.11 ml, 1.00 mmol, 1.1 eq.). After stirring at room temperature for 30 min., one drop of formic acid was added and the reaction mixture left to stir for a further 12 h at room temperature. The suspension was filtered, washed with cold ethanol and dried under reduced pressure to give L1c as a pale yellow powder (0.170 g, 51%). Compound L1c: ES mass spectrum, *m*/*z* 357 $[M+H]^+$; FABMS found 357.20791, $C_{23}H_{25}N_4$ requires 357.20792; IR (cm^{-1}): 1636 (s), 1585 (w), 1565 (w), 1466 (m), 1431 (m), 1363 (m), 1299 (m), 1257 (m), 1103 (w), 1066 (m), 1041 (w), 992 (m), 782 (s); ^1H NMR ($CDCl_3$, 293 K): δ 1.90 (s, 6H, Ar-CH_3), 2.03 (s, 6H, Ar-CH_3), 2.11 (s, 3H, (CH_3)C=N), 7.31 (m, 2H, Py-H), 7.74 (m, 2H, Py-H), 8.30 (s, 1H, CH=N), 8.31 (ddd, $^3J_{H-H}$ 7.9, $^4J_{H-H}$ 0.8, 0.9, 1H, Py-H), 8.38 (dd, $^3J_{H-H}$ 7.9, $^4J_{H-H}$ 0.8, 1H, Py-H), 8.61 (dd, $^3J_{H-H}$ 4.7, $^4J_{H-H}$ 0.8, 1H, Py-H), 8.64 (dd, $^3J_{H-H}$ 4.7, $^4J_{H-H}$ 0.8, 1H, Py-H); ^{13}C {^1H} NMR ($CDCl_3$, 293 K): δ 13.4 (Ar-CH_3), 14.0 (Ar-CH_3), 15.7 ((CH_3)C=N), 120.1 (Ar), 120.2 (Ar), 120.8 (Ar), 122.3 (Ar), 123.7 (Ar), 124.1 (Ar), 135.4 (Ar), 135.7 (Ar), 144.1 (Ar), 145.3 (Ar), 147.5 (Ar), 148.6 (Ar), 153.7 (Ar), 155.5 (Ar), 166.6 (C=N), 168.3 (C=N); m.p. = 198–201 °C.

4.3. Preparation of [(L1x)Ni_2Br_4] (**1a**–**1c**)

4.3.1. L1x = L1a (**1a**)

An oven-dried Schlenk flask equipped with a magnetic stir bar was evacuated and backfilled with nitrogen. The flask was charged with (DME)$NiBr_2$ (0.180 g, 0.58 mmol) in *n*-BuOH (10 ml) and the contents stirred at 100 °C until the nickel salt had partially dissolved. L1a was added (0.100 g, 0.29 mmol, 0.5 eq.) and the mixture was heated to 100 °C overnight. On cooling to ambient temperature, hexane was added to induce precipitation of the product. Following filtration, washing with hexane and drying under reduced pressure, **1a** was isolated as a pale green-orange solid (0.143 g, 63%). IR (cm^{-1}): 1630 (w), 1595 (s), 1567 (w), 1446 (m), 1300 (w), 1217 (m), 1155 (w), 1067 (m), 1022 (m), 977 (m), 784 (s). Anal. Calc. for $C_{22}H_{22}Br_4N_4Ni_2$: C, 33.89; H, 2.82; N, 7.19. Found: C, 34.29; H, 3.02; N, 6.68%.

4.3.2. L1x = L1b (**1b**)

Employing the method outlined in Section 4.3.1 using (DME)-$NiBr_2$ (0.170 g, 0.55 mmol), *n*-BuOH (10 ml) and L1b (0.100 g, 0.28 mmol, 0.5 eq.) at a temperature of 100 °C overnight, gave **1b** as a pale orange solid (0.156 g, 70%). Anal. Calc. for $C_{24}H_{26}Br_4N_4Ni_2$: C, 35.69; H, 3.22; N, 6.93. Found: C, 36.11; H, 3.30; N, 6.71%.

4.3.3. L1x = L1c (**1c**)

Employing the method outlined in 4.2.1. using (DME)$NiBr_2$ (0.180 g, 0.58 mmol), *n*-BuOH (10 ml) and L1c (0.100 g, 0.29 mmol, 0.5 eq.) at a temperature of 100 °C overnight, gave **1c** as a pale orange solid (0.129 g, 56%).

4.4. Preparation of [(L1a)Ni_2Cl_4] (**1d**)

An oven-dried Schlenk flask equipped with a magnetic stir bar was evacuated and backfilled with nitrogen. The flask was charged with anhydrous $NiCl_2$ (0.100 g, 0.77 mmol) in *n*-BuOH (10 ml) and the contents stirred at 100 °C for 15 min to allow partial dissolution of the nickel salt. L1a was added (0.132 g, 0.39 mmol, 0.5 eq.) and the reaction mixture stirred and heated to 100 °C overnight. On cooling to ambient temperature, hexane was added to induce precipitation of the product. Following filtration, washing

with hexane and drying under reduced pressure, **1d** was isolated as a pale orange solid (0.204 g, 68%). IR (cm^{-1}): 1635 (w), 1594 (s), 1567 (w), 1438 (m), 1310 (w), 1225 (m), 1147 (w), 1065 (m), 990 (m), 751 (s).

4.5. Preparation of $[(L1x)NiBr_2(DMF)_6]Br_2$ (**2a–2c**)

4.5.1. Lx = L1a (**2a**)

Complex **1a** (0.080 g, 0.103 mmol) was suspended in DMF (10 ml) and the mixture stirred at 90 °C for 0.5 h and filtered. On cooling to room temperature, the filtrate was layered with diethyl ether (1:3) and left to stand at room temperature. After three days, orange-red crystals of **2a** were formed (0.056 g, 45%). Compound **2a**: FAB mass spectrum, *m*/*z* 699 $[M-6DMF-Br]^+$, 620 $[M-6DMF-2Br]^+$, 538 $[M-6DMF-3Br]^+$; IR (cm^{-1}): 1645 (s), 1595 (m), 1435 (w), 1417 (w), 1385 (m), 1254 (m), 1222 (m), 1159 (w), 1102 (m), 1063 (m), 1021 (w), 775 (w). Anal. Calc. for ($C_{40}H_{64}Br_4N_{10}O_6Ni_2 \cdot DMF$): C, 40.00; H, 5.50; N, 11.94. Found: C, 39.81; H, 5.29; N, 11.71%.

4.5.2. Lx = L1b (**2b**)

Using the procedure outlined in Section 4.5.1 employing **1b** (0.075 g, 0.093 mmol), orange crystals of **2b** could be obtained (0.064 g, 55%). Compound **2b**: FAB mass spectrum, *m*/*z* 727 $[M-6DMF-Br]^+$, 645 $[M-6DMF-2Br]^+$, 567 $[M-6DMF-3Br]^+$; IR (cm^{-1}): 1646 (s), 1593 (m), 1435 (w), 1407 (w), 1380 (m), 1250 (m), 1219 (w), 1103 (m), 1065 (m), 1024 (w), 781 (m). Anal. Calc. for $C_{42}H_{68}Br_4N_{10}O_6Ni_2 \cdot 1.5DMF$: C, 41.19; H, 5.79; N, 11.88. Found: C, 40.99; H, 5.92; N, 11.67%.

4.5.3. Lx = L1c (**2c**)

Using the procedure outlined in Section 4.5.1 employing **1c** (0.075 g, 0.095 mmol), orange crystals of **2c** could be obtained (0.070 g, 60%). Compound **2c**: FAB mass spectrum, *m*/*z* 713 $[M-6DMF-Br]^+$, 633 $[M-6DMF-2Br]^+$, 553 $[M-6DMF-3Br]^+$; IR (cm^{-1}): 1643 (s), 1594 (m), 1435 (w), 1410 (w), 1374 (m), 1252 (m), 1221 (w), 1099 (m), 1063 (m), 1020 (w), 779 (m). Anal. Calc. for $C_{41}H_{66}Br_4N_{10}O_6Ni_2 \cdot 0.75DMF$: C, 40.37; H, 5.54; N, 11.71. Found: C, 40.49; H, 5.66; N, 11.60%.

4.6. Preparation of $[(L1a)Ni_2Cl_4(DMF)_4]$ (**3**)

Complex **1d** (0.075 g, 0.107 mmol) was suspended in DMF (10 ml) and the mixture stirred at 90 °C for 0.5 h and filtered. On cooling to room temperature the filtrate was layered with diethyl ether (1:3) and left to stand at room temperature. After three days, orange-red crystals of **3** could be obtained (0.047 g, 49%). Compound **3**: FAB mass spectrum, *m*/*z* 666 $[M-6DMF-Cl]^+$, 530 $[M-6DMF-2Cl]^+$, 495 $[M-6DMF-3Cl]^+$. Anal. Calc. for $C_{34}H_{50}Cl_4N_8O_4Ni_2 \cdot 0.5DMF$: C, 45.81; H, 5.75; N, 12.80. Found: C, 45.59; H, 5.61; N, 12.92%.

4.7. Screening for ethylene polymerisation

An oven-dried 200 ml Schlenk vessel equipped with magnetic stir bar was evacuated and backfilled with nitrogen. The vessel was charged with the precatalyst (0.01 mmol) and dissolved or suspended in toluene (40 ml). MAO (4.20 ml, 8.0 mmol, 800 eq.) was introduced and the reaction mixture left to stir for five min. The vessel was purged with ethylene and the contents magnetically stirred under one bar ethylene pressure at room temperature for the duration of the test. After 1 h, the test was terminated by the addition of dilute aqueous hydrogen chloride (15 ml). The polymer was filtered and dried under reduced pressure while toluene-soluble oligomers were separated and dried over magnesium sulfate. Quantitative GC analysis was performed by taking an aliquot

Table 7
Crystallographic and data processing parameters for L1a, L1c, **2a**, **2b**, **2c** and **3**

	L1a	L1c	**2a**	**2b**	**2c**		**3**
Formula	$C_{22}H_{22}N_4$	$C_{23}H_{24}N_4$	$C_{40}H_{64}Br_4N_{10}O_6Ni_2 \cdot 2DMF$	$C_{42}H_{68}Br_4N_{10}O_6Ni_2 \cdot 2DMF$	$C_{41}H_{66}Br_4N_{10}O_6Ni_2 \cdot 2DMF$		$C_{34}H_{50}Cl_4N_8O_4Ni_2 \cdot DMF$
M	342.44	356.46	1364.26	1392.32	1378.29		967.14
Crystal size (mm^3)	0.21 × 0.11 × 0.09	0.21 × 0.18 × 0.14	0.28 × 0.22 × 0.21	0.21 × 0.12 × 0.08	0.23 × 0.18 × 0.14		0.31 × 0.12 × 0.04
Crystal system	Monoclinic	Monoclinic	Triclinic	Triclinic	Triclinic		Monoclinic
Space group	*P*2(1)/*c*	*P*2(1)/*c*	*P*$\bar{1}$	*P*$\bar{1}$	*P*$\bar{1}$	*P*1	*C*2/*c*
a (Å)	10.497(6)	9.1204(13)	9.6479(15)	9.5814(16)	9.5735(14)		24.280(6)
b (Å)	9.208(6)	9.0489(13)	11.4550(17)	11.843(2)	11.7095(17)		15.699(4)
c (Å)	9.273(6)	11.9457(17)	13.926(2)	13.901(2)	14.041(2)		13.220(3)
α (°)	90	90	72.654(2)	76.411(3)	75.021(3)		90
β (°)	101.821(12)	108.518(3)	82.197(3)	80.959(3)	80.571(3)		109.090(4)
χ (°)	90	90	79.326(3)	77.932(3)	77.588(3)		90
U ($Å^3$)	877.3(9)	934.8(2)	1438.3(4)	1489.6(4)	1475.1(4)		4762(2)
Z	2	2	1	1	1		4
D_c ($Mg\ m^{-3}$)	1.296	1.266	1.575	1.552	1.522		1.349
F(000)	364	380	698	714	706		2024
μ(Mo Kα) (mm^{-1})	0.079	0.077	3.491	3.373	3.405		1.063
Reflections collected	5514	6557	10511	11655	11626	10719	18181
Independent reflections	1533	1642	5041	5769	5742	9375	4679
R_{int}	0.0719	0.0706	0.0479	0.0446	0.0320	0.0215	0.0448
Restraints/parameters	0/120	0/130	0/335	0/345	0/308	3/350	0/241
Final *R* indices $[I > 2\sigma(I)]$	R_1 = 0.0461	R_1 = 0.0523	R_1 = 0.0466	R_1 = 0.0514	R_1 = 0.0576	R_1 = 0.0633	R_1 = 0.0477
	wR_2 = 0.0986	wR_2 = 0.1182	wR_2 = 0.1080	wR_2 = 0.1032	wR_2 = 0.1392	wR_2 = 0.1537	wR_2 = 0.1202
All data	R_1 = 0.0598	R_1 = 0.0797	R_1 = 0.0656	R_1 = 0.0836	R_1 = 0.0885	R_1 = 0.0960	R_1 = 0.0616
	wR_2 = 0.1042	wR_2 = 0.1387	wR_2 = 0.1141	wR_2 = 0.1125	wR_2 = 0.1517	wR_2 = 0.1737	wR_2 = 0.1256
Goodness-of-fit on F^2	1.047	0.993	0.942	0.923	0.968	0.988	0.994

Data in common: temperature 150(2) K, graphite-monochromated Mo Kα radiation, λ = 0.71073 Å; $R_1 = \sum||F_o| - |F_c||/\sum|F_o|$, $wR_2 = [\sum w(F_o^2 - F_c^2)^2 / \sum w(F_o^2)^2]^{1/2}$, $w^{-1} = [\sigma^2(F_o)^2 + (aP)^2]$, $P = [\max(F_o^2, 0) + 2(F_c^2)]/3$ where *a* is a constant adjusted by the program; goodness of fit $= [\sum(F_o^2 - F_c^2)2/(n-p)]^{1/2}$, where *n* is the number of reflections and *p* the number of parameters.

of the solution containing a weighed amount of a standard (*n*-heptadecene). For analysis of the oligomers by NMR (^{1}H and ^{13}C) spectroscopy, the solvent was removed on the rotary evaporator and the residue dissolved in $CDCl_3$.

4.8. Crystallography

Data for L1a, L1c, **2a**, **2b**, **2c** and **3** were collected on a Bruker APEX2000CCD diffractometer. Details of data collection, refinement and crystal data are listed in Table 7. The data were corrected for Lorentz and polarisation effects and empirical absorption corrections applied. Structure solution by direct methods (and Patterson methods) and structure refinement using full matrix least squares on F^2 employed SHELXTL version 6.10 [21]. Hydrogen atoms were included in calculated positions (C–H = 0.96 Å) riding on the bonded atom with isotropic displacement parameters set to 1.5 Ueq(C) for methyl H atoms and 1.2 Ueq(C) for all other H atoms. All non-H atoms were refined with anisotropic displacement parameters. Disordered solvent was omitted using the SQUEEZE option in platon for **2c** and **3**.

Acknowledgement

We thank the University of Leicester and ExxonMobil (to J.D.A.P.) for financial assistance.

Appendix A. Supplementary material

CCDC 680732, 680733, 680734, 680735, 680736, 680737 and 680738 contain the supplementary crystallographic data for this paper. These data can be obtained free of charge from The Cambridge Crystallographic Data Centre via www.ccdc.cam.ac.uk/data_request/cif. Supplementary data associated with this article can be found, in the online version, at doi:10.1016/j.jorganchem.2008.05.020.

References

[1] M. Shibasaki, Y. Yamamoto (Eds.), Multimetallic Catalysts in Organic Synthesis, Wiley–VCH Verlag GmbH & Co. KGaA, Weinheim, Germany, 2004.
[2] See for example (a) B.M. Trost, A. Fettes, B.T. Shireman, J. Am. Chem. Soc. 126 (2004) 2660;
(b) B.M. Trost, H. Ito, E.R. Silcoff, J. Am. Chem. Soc. 123 (2001) 3367;
(c) B.M. Trost, A.H. Weiss, A.J. von Wangelin, J. Am. Chem. Soc. 128 (2006) 8.
[3] (a) L.E. Breyfigle, C.K. Williams, V.G. Young Jr., M.A. Hillmyer, W. Tolman, Dalton Trans. (2006) 928;
(b) B.Y. Lee, H.Y. Kwon, S.Y. Lee, S.J. Na, S.-I. Han, H. Yun, H. Lee, Y.-W. Park, J. Am. Chem. Soc. 127 (2005) 3031;
(c) C.K. Williams, N.R. Brooks, M.A. Hillmyer, W.B. Tolman, Chem. Commun. (2002) 2132;
(d) E. Bukhaltsev, L. Frish, Y. Cohen, A. Vigalok, Org. Lett. 7 (2005) 5123;
(e) M.L. Hlavinka, M.J. McNevin, R. Shoemaker, J.R. Hagadorn, Inorg. Chem. 45 (2006) 1815. and refs therein;
(f) Y.D.M. Champouret, W.J. Nodes, J.A. Scrimshire, K. Singh, G.A. Solan, I. Young, Dalton Trans. (2007) 4565.
[4] (a) M.L. Hlavinka, J.R. Hagadorn, Organometallics 24 (2005) 5335;
(b) M.L. Hlavinka, J.R. Hagadorn, Chem. Commun. (2003) 2686;
(c) B.C. Clare, N. Sarker, R. Shoemaker, J.R. Hagadorn, Inorg. Chem. 43 (2004) 1159;
(d) M.L. Hlavinka, J.R. Hagadorn, Organometallics 24 (2005) 4116.
[5] (a) H. Li, C.L. Stern, T.J. Marks, Macromolecules 38 (2005) 9015;
(b) H. Li, L. Li, D.J. Schwartz, M.V. Metz, T.J. Marks, L. Liable-Sands, A.L. Rheingold, J. Am. Chem. Soc. 127 (2005) 14756;
(c) N. Guo, L. Li, T.J. Marks, J. Am. Chem. Soc. 126 (2004) 6542;
(d) S.K. Noh, M. Lee, D.H. Kum, K. Kim, W.S. Lyoo, D.-H. Lee, J. Polym. Sci. Part A: Polym. Chem. 42 (2004) 1712.
[6] (a) C. Redshaw, M.A. Brown, L. Warford, D.M. Homden, A. Arbaoui, M.R.J. Elsegood, S.H. Dale, T. Yamato, C.P. Casas, S. Matsui, S. Matsuura, Chem. Eur. J. 13 (2007) 1090;
(b) X. Yan, A. Chernega, M.L.H. Green, J. Sanders, J. Souter, T. Ushioda, J. Mol. Catal. A: Chem. 128 (1998) 119;
(c) G. Desurmont, Y. Li, H. Yasuda, T. Maruo, N. Kanehisa, Y. Kai, Organometallics 19 (2000) 1811;
(d) S.K. Noh, J. Kim, J. Jung, C.S. Ra, D.-H. Lee, H.B. Lee, S.W. Lee, W.S. Huh, J. Organomet. Chem. 580 (1999) 90;
(e) G.M. Diamond, A.N. Chernega, P. Mountford, M.L.H. Green, J. Chem. Soc., Dalton Trans. (1996) 921;
(f) S.A. Larkin, J.T. Golden, P.J. Shapiro, G.P.A. Yap, D.M.J. Foo, A.L. Rheingold, Organometallics 15 (1996) 2393;
(g) J. Huang, Z. Feng, H. Wang, Y. Qian, J. Sun, Y. Xu, W. Chen, G. Zheng, J. Mol. Catal. A: Chem. 189 (2002) 187;
(h) J. Jung, S.K. Noh, D.-H. Lee, S.K. Park, K. Kim, J. Organomet. Chem. 595 (2000) 147;
(i) M. Mitani, K. Oouchi, M. Hayakawa, T. Yamada, T. Mukaiyama, Polym. Bull. 35 (1995) 677;
(j) X. Liu, J. Sun, H. Zhang, X. Xiao, F. Lin, Eur. Polym. J. 41 (2005) 1519.
[7] (a) T. Hu, L.-M. Tang, X.-F. Li, Y.-S. Li, N.-H. Hu, Organometallics 24 (2005) 2628;
(b) J.-P. Taquet, O. Siri, P. Braunstein, R. Welter, Inorg. Chem. 45 (2006) 4668;
(c) D. Zhang, G.-X. Jin, Organometallics 22 (2003) 2851;
(d) H.-K. Luo, H. Schumann, J. Mol. Cat. A: Chem. 227 (2005) 153;
(e) X. Mi, Z. Ma, L. Wang, Y. Ke, Y. Hu, Macromol. Chem. Phys. 204 (2003) 868;
(f) S. Zhang, W.-H. Sun, X. Kuang, I. Vystorop, J. Yi, J. Organomet. Chem. 692 (2007) 5307;
(g) A. Tomov, K. Kurtev, J. Mol. Cat. A: Chem. 103 (1995) 95;
(h) K. Kurtev, A. Tomov, J. Mol. Cat. A: Chem. 88 (1994) 141;
(i) P. Wehrmann, S. Mecking, Organometallics 27 (2008) 1399;
(j) M. Tanabiki, K. Tsuchiya, Y. Motoyama, H. Nagashima, Chem. Commun. (2005) 3409.
[8] (a) G.A. Solan, J.D.A. Pelletier, PCT Int. Appl., 2005, WO 2005118605;
(b) R.E. Murray, U.S. Pat. Appl. Publ., 2004, US 2004054150.
[9] J. Kuwabara, D. Takeuchi, K. Osakada, Chem. Commun. (2006) 3815.
[10] (a) T.V. Laine, M. Klinga, M. Leskela, Eur. J. Inorg. Chem. (1999) 959;
(b) T.V. Laine, U. Piironen, K. Lappalainen, M. Klinga, E. Aitola, M. Leskela, J. Organomet. Chem. 606 (2000) 112;
(c) G.J.P. Britovsek, S.P.D. Baugh, O. Hoarau, V.C. Gibson, D.F. Wass, A.J.P. White, D.J. Williams, Inorg. Chim. Acta 345 (2003) 279;
(d) T.V. Laine, K. Lappalainen, J. Liimatta, E. Aitola, B. Lofgren, M. Leskala, Macromol. Rapid Commun. 20 (1999) 487;
(e) S.P. Meneghetti, P.G. Lutz, J. Kress, Organometallics 18 (1999) 2734;
(f) A. Koppl, H.G. Alt, J. Mol. Catal. A: Chem. 154 (2000) 45.
[11] (a) Y.D.M. Champouret, J. Fawcett, W.J. Nodes, K. Singh, G.A. Solan, Inorg. Chem. 45 (2006) 9890;
(b) S. Jie, D. Zhang, T. Zhang, W.-H. Sun, J. Chen, Q. Ren, D. Liu, G. Zheng, W. Chen, J. Organomet. Chem. 690 (2005) 1739;
(c) V.C. Gibson, C.M. Halliwell, N.J. Long, P.J. Oxford, A.M. Smith, A.J.P. White, D.J. Williams, Dalton Trans. (2003) 918.
[12] For use of 1,4-phenylene-linked derivatives see (a) A. Singh, M. Chandra, A.N. Sahay, D.S. Pandey, K.K. Pandey, S.M. Mobin, M.C. Puerta, P. Valerga, J. Organomet. Chem. 689 (2004) 1821;
(b) H.-C. Wu, P. Thanasekaran, C.-H. Tsai, J.-Y. Wu, S.-M. Huang, Y.-S. Wen, K.-L. Lu, Inorg. Chem. 45 (2006) 295;
(c) M. Barboiu, E. Petit, A. van der Lee, G. Vaughan, Inorg. Chem. 45 (2006) 484;
(d) N.M. Shavaleev, Z.R. Bell, G. Accorsi, M.D. Ward, Inorg. Chim. Acta 351 (2003) 159;
(e) N. Yoshida, K. Ichikawa, M. Shiro, J. Chem. Soc., Perkin Trans. 2 (2000) 17.
[13] For the importance of steric bulk in late transition metal catalysis see (a) V.C. Gibson, C. Redshaw, G.A. Solan, Chem. Rev. 107 (2007) 1745;
(b) V.C. Gibson, S. Spitzmesser, Chem. Rev. 103 (2003) 283;
(c) S.D. Ittel, L.K. Johnson, M. Brookhart, Chem. Rev. 100 (2000) 1169.
[14] (a) N. Chanda, B. Mondal, V.G. Puranik, G.K. Lahiri, Polyhedron 21 (2002) 2033;
(b) P.J. Ball, T.R. Shtoyko, J.A.K. Bauer, W.J. Oldham, W.B. Connick, Inorg. Chem. 43 (2004) 622.
[15] A. Gerli, K.S. Hagen, L.G. Marzilli, Inorg. Chem. 30 (1991) 4673.
[16] For use of the ν(CO) stretch as a guide to relative donor capability of imines/pyridine see (a) M. Brockmann, H. tom Dieck, J. Klaus, J. Organomet. Chem. 301 (1986) 209;
(b) S. Morton, J.F. Nixon, J. Organomet. Chem. 282 (1985) 123;
(c) L. Gonsalvi, J.A. Gaunt, H. Adams, A. Castro, G.J. Sunley, A. Haynes, Organometallics 22 (2003) 1047.
[17] (a) T. Usami, S. Takayama, Macromolecules 17 (1984) 1756;
(b) G.B. Galland, R.F. de Souza, R.S. Mauler, F.F. Nunes, Macromolecules 32 (1999) 1620;
(c) L.P. Linderman, N.O. Adams, Anal. Chem. 43 (1971) 1245;
(d) M. De Pooter, P.B. Smith, K.K. Dohrer, K.F. Bennett, M.D. Meadows, C.G. Smith, H.P. Schouwenaars, R.A. Geerards, J. Appl. Polym. Sci. 42 (1991) 399.
[18] W.L.F. Armarego, D.D. Perrin, Purification of Laboratory Chemicals, 4th ed., Butterworth Heinemann, 1996.
[19] F.E. Mabbs, D.J. Machin, Magnetism and Transition Metal Complexes, Chapman and Hall, London, 1973.
[20] (a) C.J. O'Connor, Prog. Inorg. Chem. 29 (1982) 203;
(b) R.C. Weast (Ed.), Handbook of Chemistry and Physics, 70th ed., CRC Press, Boca Raton, FL, 1990. p. E134.
[21] G.M. Sheldrick, SHELXTL Version 6.10. Bruker AXS Inc., Madison, WI, USA, 2000.